VOL. 10, NO 21, NOVEMBER, 2015 ISSN 1819-6608
ARPN Journal of Engineering and Applied Sciences

www.arpnjournals.com

DESIGN AND OPTIMIZATION OF LOW SPEED HORIZONTAL-AXIS WIND TURBINE USING OPENFOAM

Dena Hendriana[1], Tommy Firmansyah[1], Joga Dharma Setiawan[2] and Dodi Garinto[3]
[1]Center for Computational Fluid Dynamics Surya University, Indonesia
[2]Department of Mechanical Engineering, Universiti Teknologi Petronas, Malaysia
[3]Electric Propulsion Center, Surya University, Indonesia
E-Mail: joga.setiawan@petronas.com.my

ABSTRACT

This paper presents a design and optimization of 7.5 m diameter, 6-bladed horizontal-axis wind turbine designed for low speed wind of 4 m/s; using opens source Computational Fluid Dynamics (CFD) software OpenFOAM. The blade configuration was chosen to be as simple as possible such that manufacturing cost can be reduced. In the simulations, a solver called simpleFoam based on the Reynolds Averaged Navier-Stokes (RANS) with k-ω turbulence model and steady-state solution method is used. For validating both drag and torque calculations, three different validation cases were carried out and compared to popularly known experimental results. This validation study shows that by utilizing fine mesh resolutions the numerical errors associated with CFD solutions could be minimized to merely 2-4% compared to the experimental results. Optimization study was then conducted by varying the width of the blade, inclination angle of the outer tip of the blade, and inclination angle of the inner tip of the blade. This optimization yields power efficiency between 38-41%. After a series of geometry fine tunings, the best modification was found at 52% power efficiency. It was found that variation of wind speed had little effect to the power efficiency but it varied the maximum power. On the other hand, the wind angle to wind turbine axis contributes very strong impact to the power efficiency.

Keywords: wind turbine, power efficiency, CFD software, RANS.

INTRODUCTION

The use of CFD in designing wind turbines has been performed by a number of researchers in the past. Sezer-Uzol and Long [1], did CFD analysis using LES for a horizontal-axis wind turbine with 2 blades called NREL. Gomez-Iradi and Barakos [2] did similar CFD analysis with a 2-bladed NREL wind turbine, but used RANS CFD method. Impacts of both root and tip of the blade, aspect ratio, and pitch angle were investigated. Their CFD results showed that the effect of blade aspect ratio and pitch angle was larger to thrust and energy level than that of the blade root and tip. Meanwhile, Ferreira *et al* [3] employed RANS CFD to study a 2D wind turbine with vertical axis using NACA0015 airfoil. This study in particular looked at the impact of various turbulence models and compared the results with experimental data from Particle Image Velocimetry (PIV) and also the impact of grid resolution to accuracy level. Kaminsky *et al* [4] also did a similar study with NACA001234 using RANS CFD method. In their work, aerodynamic performance of the 2D airfoil was first calculated before full wind turbine assembly simulation. The analysis was carried out for a number of yaw angles and wind speed.

The work in this paper uses the fact that the average wind speed in some tropical countries, such as Indonesia, is in a range of 4-5 m/s [5] even though in areas along coastline the wind speed could reach as much as 10 m/s. Thus, the wind speed of 4 m/s is considered in this paper with emphasizing on the capability of free CFD software namely OpenFOAM for development of wind turbine blade. The optimization in this study is performed in a simple and manual way that later can be improved by applying the optimization method as done in references [6, 7, 8].

Wind turbine geometry

The geometry of horizontal-axis wind turbine used in the present work is shown in Figure 1. It is based on the popular horizontal-axis wind turbine with 6 blades designed to achieve high energy efficiency at relatively low wind speed. This requires quite a large diameter of 7.5 m using the average wind speed of 4 m/s to attain around 850 watts power generation.

The blade shape was made in simple form which is a plate without airfoil for reduced manufacturing cost consideration. In this paper, 3 different variables of geometry were investigated with different rotating speeds to achieve highest possible power. All simulations produced torque τ in Newton-meter and Power calculated by simply multiplying the torque with rotating speed τ.ω. The most optimum power was acquired from a combination of 3 geometry variables at a certain rotating speed. The three different geometry variables were blade width, outer tip angle and inner tip angle. Figure 2 shows 4 different blade widths considered. The blade widths covered 25%, 50%, 75% and 100% of the rotor swept area from front-view.

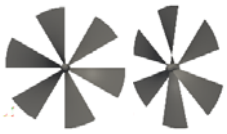

Figure-1. Geometry of 6-bladed wind turbine to be optimised (2 different angles of view).

(a) (b) (c) (d)

Figure-2. (a) blade width covering 25% frontal area, (b) 50%, (c) 75% dan (d) 100%

The second variable is the outer tip angle measured from the horizontal axis. Figure 3 shows 3 different angles, 81º, 84º and 87º. Note that the tip angle does not change the overall coverage percentage of the swept area. These angles were already close to the optimum range.

The third variable is the inner tip angle which is also measured from the horizontal axis. Figure-4 shows 3 different angles considered, i.e. 12.2º, 14.5º and 17.9º. Similarly, this angle does not change the overall coverage of the swept area.

CFD simulation method

The analysis was performed with RANS CFD method using open source CFD software called OpenFOAM, see Ref. [10]. It was chosen because the software has been undergoing lots of tests and validations among the CFD community worldwide with good accuracy. Moreover, the open base software also gives opportunities for development and improvement beside it is a free software license.

OpenFOAM CFD software

Incompressible solver based on Reynolds Averaged Navier-Stokes (RANS) with k-ω turbulence model (kOmegaSST) and steady-state solution method was used together withthe solver in OpenFOAM namely simpleFoam.

In Navier-Stokes equations the convective part is always dominant for problems with high Reynolds number (Re). This convective part is usually termed as the divergence component in OpenFOAM. For this reason, several models had been tested with high order accuracy such as: linearUpwind, SFCD, vanLeer, MUSCL, QUICKV, GammaV. However, all did not produce numerical stability with either unrealistically high or negative values of turbulent components, k and omega. Therefore, to overcome this issue the "bounded Gauss upwind" with first order accuracy for divergence component was used instead.

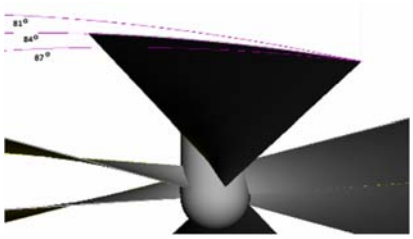

Figure-3. Outer tip angles, 81^0, 84^0 and 87^0.

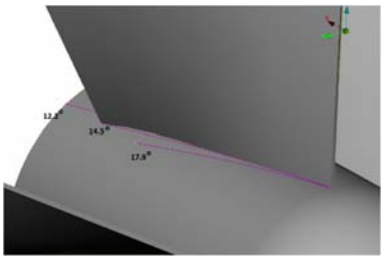

Figure-4. Inner tip angles, 12.2º, 14.5º, dan 17.9º.

To represent rotating movement of the wind turbine an MRF (Multi Reference Frame) model was adopted. A predefined cylindrical volume that represents the rotating regime was required. Then the magnitude and rotating direction of the MRF zone was defined in "fvOption" file.

Prior to simulation some specific conditions namely Boundary Conditions need to be defined. For the simulations here the rotating speed and air property were specified. Figure-5 shows simulation set-up with 4 m/s wind speed and turbulence intensity of 5%.

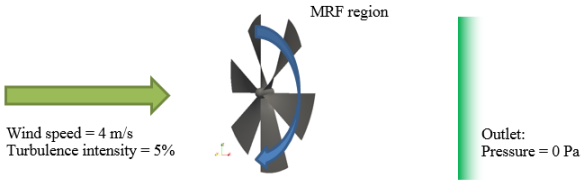

Figure-5. Simulation condition for CFD analysis.

The simulations were conducted with geometry input, wind speed and MRF rotating speed defined to calculate the resulting wind turbine torque at steady-state solution. Wind turbine power was calculated by multiplying the torque with the speed of rotation.

When the geometry preparation was ready, computational mesh was generated using an OpenFOAM utility called snappy HexMesh. The geometry was imported in STL format and then the 3D cells were

generated with predominantly hexahedral and split-hexahedral typed mesh. To achieve high accuracy of solution, fine mesh resolution was placed near the surfaces of the wind turbine. For good simulation results, 4 to 12 millions computational cells were required depending on the blade width. The cell size near to the surfaces was 6.25 mm with one cell of 1.25 mm thickness boundary layer attached. However, the automatic boundary layer generation by snappyHexMesh was not consistent across all surfaces and some areas did not have boundary layer. Nevertheless the wall y+ near to the surfaces was around 18 in average, which is quite low considering the low wind speed of 4 m/s. The mesh distribution is shown in Figure 6.All CFD simulations were conducted on a high-performance server with 32-core CPU with 128 GB RAM.

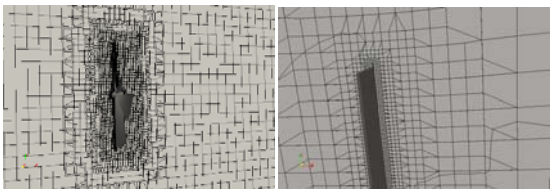

Figure-6. Global GridMesh and detailed grid mesh near the blade surfaces.

Validation program of OpenFOAM

To gain confidence in the accuracy of OpenFOAM simulations of the wind turbine, a number of validation simulations on the simple Foam module with k-ω SST turbulence model and steady-state solution were carried out. The results from this validation study were compared to the popularly known values of C_d [11]. Moreover, the validation simulations were also performed with three different mesh configurations to show whether the solutions were already mesh-independent. The three mesh configurations represent coarse, medium and fine resolutions. Coarse means the number of computational cells are relatively small with large cell sizes whilst the fine means high cell numbers with relatively small cell sizes.

There were three validation cases. The first two cases were validating drag calculation and the final one for torque validation. Figure 7 shows these three cases. For the first case, the wind speed of 4 m/s is blowing at a hollow hemisphere with diameter of 1.0 m facing stream. In this case, the drag caused by the hemisphere was compared the known value of C_d at 0.38[11]. In the second case, the open end of the hemisphere is facing the stream. The known value for the C_d in this caseis 1.42 [11].

For the third case, both hemispheres at 2.0 m apart were combined creating a wind turbine look-alike, connected with a 10 mm-diameter pipe. These combined objects were assumed on static positions and CFD simulations were conducted to calculate both drag and torque at the pipe center and the results were then compared with individual drag and torque from each hemisphere separately.

Figure-8 depicts simulation results for case 1 using 3 different mesh configurations (coarse, medium and fine) with comparison from experiment (C_d = 0.38). The graph shows that the higher the mesh resolution the more accurate the CFD solution and medium to fine mesh configurations produced good results. In general, the more computational cells used the more computational resources are required and hence the more accurate the CFD solutions.

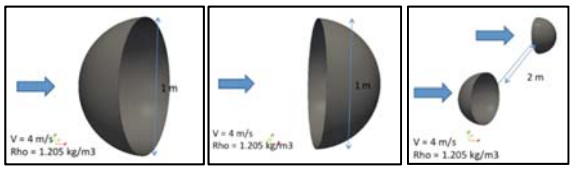

(a) (b) (c)

Figure-7. Validation cases: (a) case 1, hollow hemisphere facing stream. (b) case 2, open end of hemisphere facing stream. (c) case 3, combined hemispheres look alike a wind-turbine.

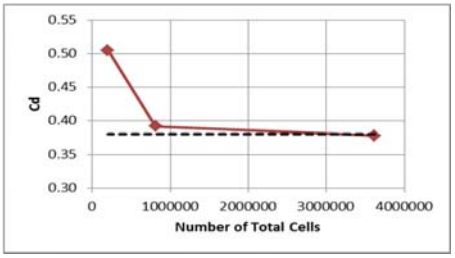

Figure-8. Resulting drag for case 1 compared to known value 0.8 [11] (dashed line).

Similar graph is produced in Figure-9 showing the simulation results for case 2 with 3 different mesh sizes and their comparisons with experimental value of C_d (=1.42). This graph demonstrates that implementing fine mesh resolution has led to a very small error of less than 2%.

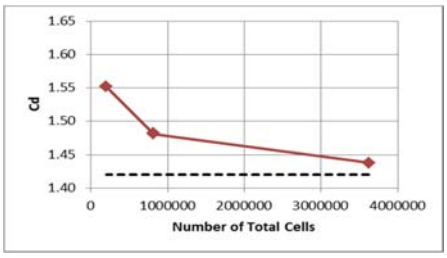

Figure-9. Resulting drag for case 2 compared to known value 1.42 [11] (dashed line).

For case 3 no experimental result is available for the combined hemispheres and therefore comparison is made based on individual drag from each hemisphere and one connecting pipe with assumption that they did not interact with one another. Figure-10 shows these comparisons and as with the previous cases finer mesh resolution improved the results significantly. The finest mesh produced CFD solution that differed less than 4% with estimated experimental value.

Resulting torques for case 3 and their comparison with experiment are shown in Figure-11. It is obvious that the predicted torques from all 3 mesh sizes were very close with experiment. This gives confidence on the accuracy of OpenFOAM to predict torque. What was interesting was that even the coarse mesh already gave close torque prediction to the experiment and on the other hand, the predicted drags were not that close to the experiment. This can be explained as follows. The inaccuracy of force calculation for the hemisphere facing forward could be compensated by another inaccuracy produced by the rearward facing hemisphere.

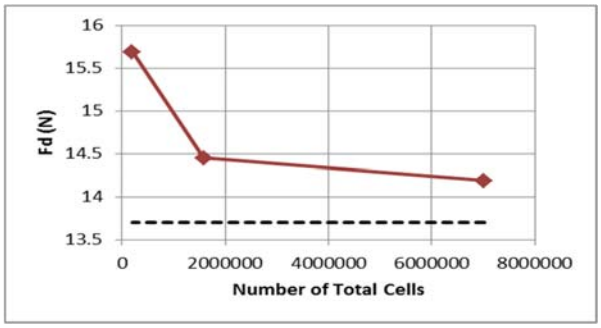

Figure-10. Resulting drag from case 3 compared with estimated experiment (dashed line).

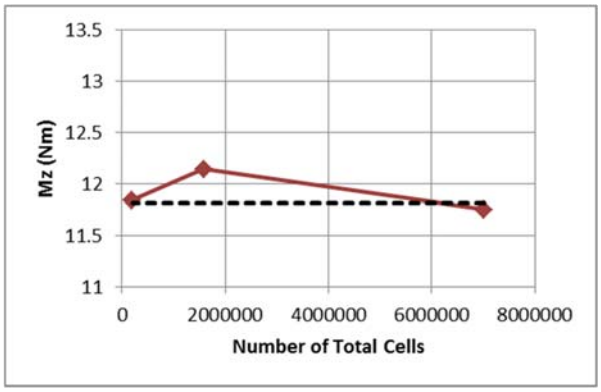

Figure-11. Resulting torque for case 3 compared with estimation from experiment (dashed line).

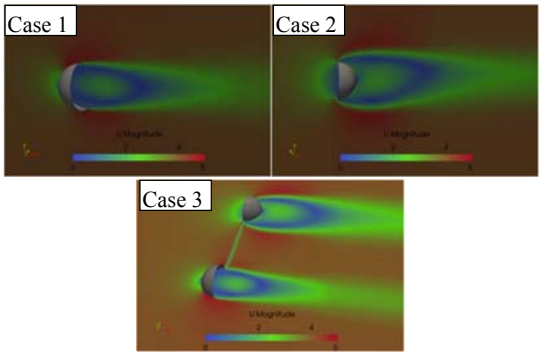

Figure-12. Wind speed distribution for cases 1 to3.

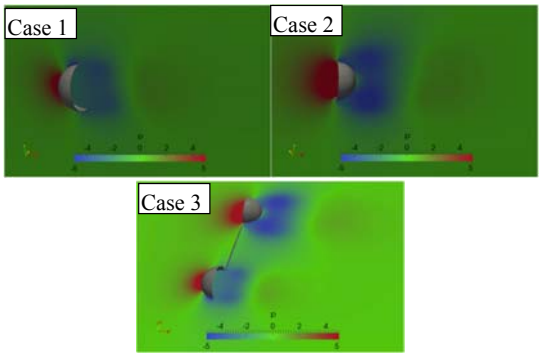

Figure-13. Pressure distribution for cases 1to 3.

The common trend from the above three cases was that the more the computational cells used the more accurate the simulation results and the use of fine mesh consistently produced good accuracy.All simulation results for cases 1-3 can be seen in Figures 12-13 for velocity and pressure distributions, consecutively.

Optimization of wind turbine with CFD analysis

For optimizing the wind turbine the same CFD method used on the validation cases was also implemented. simpleFoam solver with incompressible, k-ω SST turbulence model and steady-state solution was used with MRF approach to simulate the rotating regime. The fine mesh resolution similar to those in the validation cases was applied. Optimization was done by finding the maximum power/energy resulted from the wind turbine as a function of varied geometric parameters as described in section 2: rotating speed, blade width, outer tip angle and inner tip angle.

The search for maximum power was done by using linear approach from a base configuration with its parameters closed to known optimal design. The base configuration parameters are blade width of 50% frontal coverage, the outer tip angle of 84^o and inner tip angle of 14.5^o.

During optimization, for every configuration, four different simulations were performed with different rotating speeds to obtain maximum power as a function of rotating speeds. The optimization was done by finding an optimum combination of rotating speed, blade width and outer tip angle and then the optimization work continued with finding out the optimum inner tip angle. Results from this parametric study are discussed below including impacts from each parameter change to the flows across the wind turbine.

Base configuration results

The power and torque produced by the wind turbine as a function of rotating speed is shown Figure-14. It was found that the maximum power occurred at around 30 RPM while the maximum torque produced when the rotating speed was between 10-20 RPM. The maximum power usually takes place at the middle of operating rotating speeds, i.e. 0-60 RPM, which agrees well with the simulation results. However, the maximum torque normally happens at 0 RPM, which is contrary to the simulation results that indicate the declining torque at 0 RPM. This can be explained by examining Figures-15 and16, which show the pressure distribution at the top and bottom surfaces of the wind turbine blade. The pressure at the top surface at 0 RPM is higher than at the one at20 RPM due to higher imparted air pressure. On the other hand, at the bottom surface the pressure at 0 RPM is higher than the one at 20 RPM. For the bottom surface the lower the pressure the higher the torque is produced. That is why the torque at 20 RPM was higher. At 0 RPM the "stall" condition led the pressure at the bottom surface higher. Figure-14 shows this "stall" at 0 RPM where the air speed was high between the blades, and low at the back of the blades.

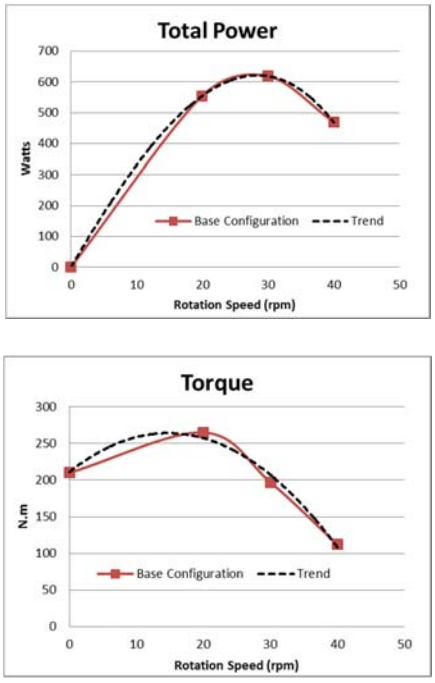

Figure-14. Power and torque for the base configuration.

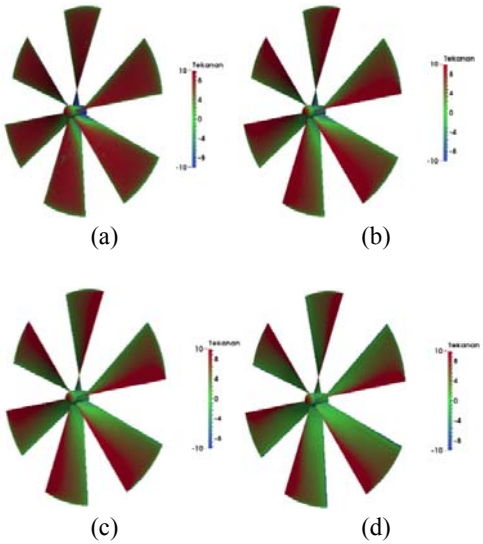

Figure-15. Base configuration result: Pressure distribution at the front surface of the blades for (a) 0 rpm, (b) 20 rpm, (c) 30 rpm, (d) 40 rpm.

Figures 15-17 show that the higher the RPM the lower the pressure at the front surface of the blades, the higher the pressure at the rear surface (except at 0 RPM due to "stall") and the higher the air speed at the back of the blades. This demonstrates that the higher the RPM the lower the torque generated.

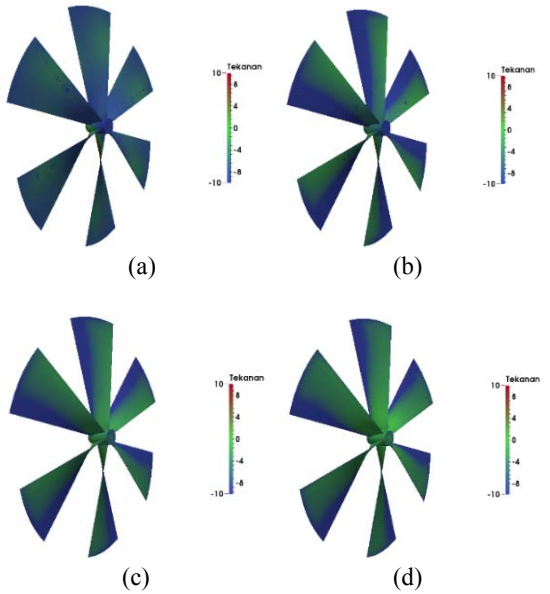

Figure-16. Base configuration result: Pressure distribution at the rear surface of the blades for (a) 0 rpm, (b) 20 rpm, (c) 30 rpm, (d) 40 rpm.

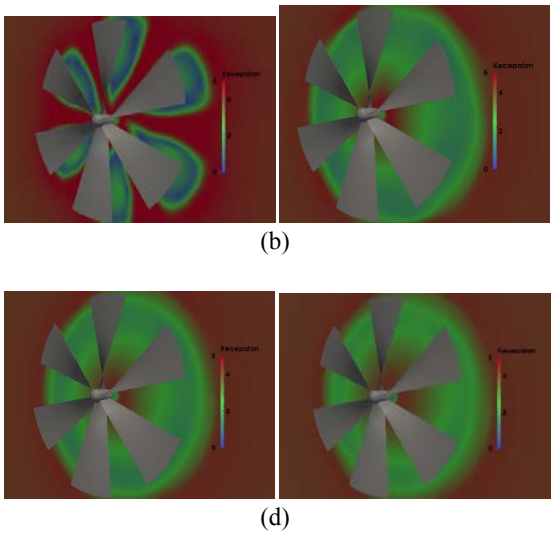

Figure-17. Base Configuration result: Velocity distribution 0.5 m upstream of the blades for (a) 0 rpm, (b) 20 rpm,
(c) 30 rpm, (d) 40 rpm.

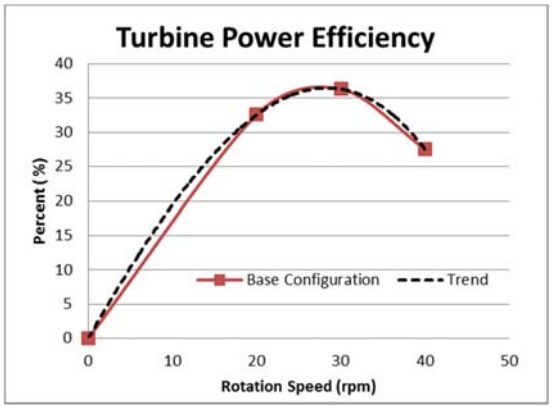

Figure-18. Wind turbine efficiency for the base configuration.

Using the efficiency definition [9] with a proportion of output power of the wind turbine to the incoming air kinetic energy, it can be seen at Figure-18 that the peak efficiency for the base configuration occurred at about 28 RPM with energy efficiency of around 36%.

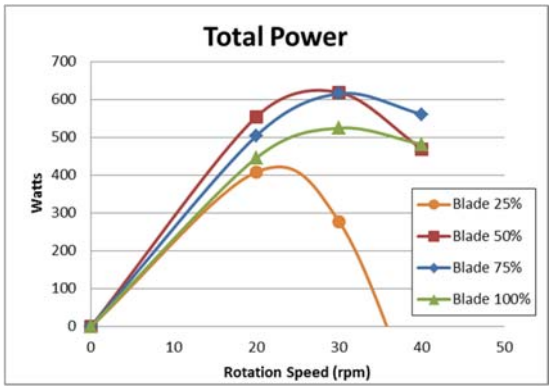

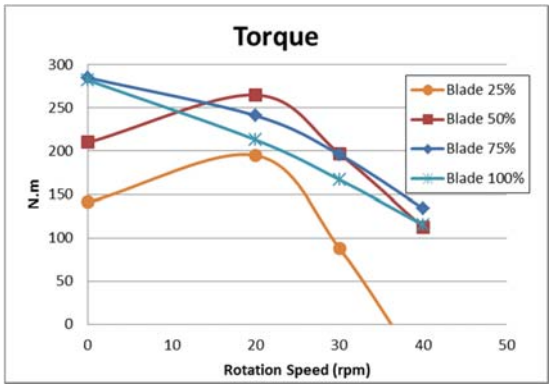

Figure-19. Power and torque as a function of rotating speeds for various blade widths.

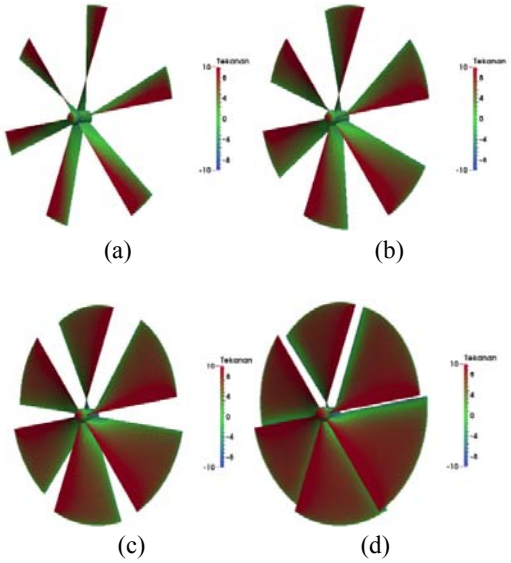

Figure-20. Pressure distribution at the front surface at peak power condition (a) width 25%, (b) width 50%, (c) width 75%, (d) width 100%.

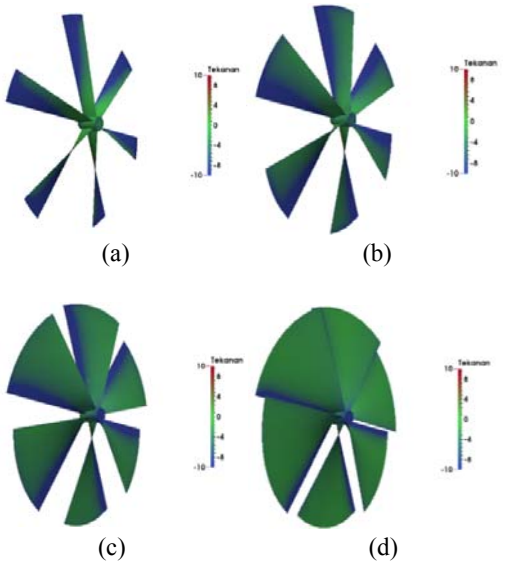

Figure-21. Pressure distribution at the rear surface of the blade at the peak-power condition for (a) width 25%, (b) width 50%, (c) width 75%, (d) width 100%.

Optimization results for blade width parameter

The blades width were varied to give 25%, 50%, 75% and 100% frontal coverage as shown in Figure-19 for 4 different blade width configurations. The outer tip angle of 84º and inner tip angle of 14.5ºwerekept constant. The power and torque produced by the wind turbine were calculated for 4 different rotating speeds: 0, 20, 30 and 40 RPM. Figure-4.2.1 shows power and torque as a function of rotating speed for different blade widths. From the graphs, it can be seen that maximum powers for all blade widths are within 20-30 RPM and the maximum power was achieved for the 50% blade width. It was also revealed that the minimum torque and power occurred when the blade width was 25%.

Figures 20-22showcomparison of simulation results for various blade widths at around maximum power. For the 25% width the rotating speed was at 20 RPM, while the 50%, 75%, and 100% widthswasat30 RPM.

Figures 20-22demonstratethat the power and torque resulted from 100% blade width were smaller than that of 75%. Although the area at the front surface of 100% width was wider and had higher pressure than that of 75% the pressure at the rear surface of the blade was also higher and thus led to decreased wind turbine efficiency. The lower wind speed at the rear surface of the 100% width was also indicated that the wind flow across the swept area was lower and thus led to lower total kinetic energy due to low air mass inflow. Figure 22 shows that the 25% width still produced high wind speed at the rear surface of the blade whilst the 75% and 100% widths produced very low wind speed. The 50% width turned out to give the medium wind speed and hence most optimum.

Figure-23 shows efficiencies for all blade widths and that the highest efficiency value of 36% achieved when the 50% width rotated at 28 RPM, which is the same as the Base Configuration.

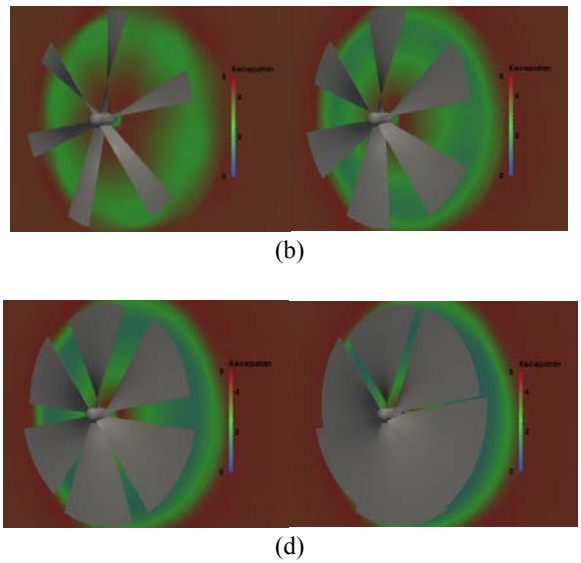

Figure-22. Wind speed distribution at 0.5 m downstream of the wind turbine at the peak-power for (a) width 25%, (b) width 50%, (c) width 75%, (d) width 100%.

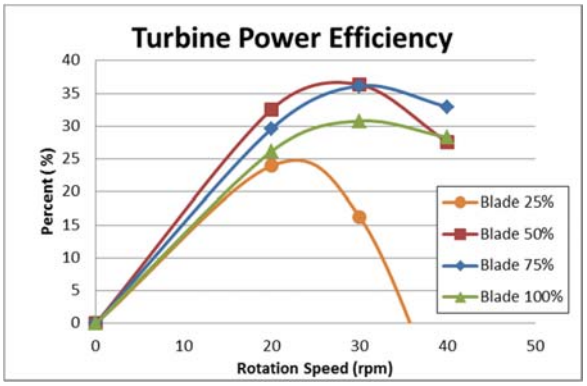

Figure-23. Wind turbine efficiency for different blade.

Optimization results for outer tip angle parameter

The parameter changed in this optimization study was the outer blade tip angle with varied angles of 81^0, 84^0 and 87^0, as depicted in Figure-24. The 50% blade width was used with inner blade tip angle of 14.5^0 as constant. Power and Torque generated by the wind turbine as a function of outer blade tip angle were simulated using 4 different rotating speeds; 0, 20, 30 and 40 RPM.

Figure-24 shows Power and Torque graphs as a function of outer blade tip angle for different rotating speeds. The maximum power achieved within a range of 25-30 RPM and at the outer blade tip angle of 81^o. Configuration with outer blade tip angle of 87^o gave the lowest maximum power and torque.

Figure-25 shows the wind turbine efficiencies for all outer blade tip angles and the highest efficiency of 38% achieved at the outer tip angle of 81^0 and 25 RPM rotating speed. The efficiencies at 81^0 and 84^0wereso close, which indicates that the optimum value has been or was almost reached.

Further improvement of wind turbine performance

Following the finding of optimum configuration from a combination of blade width, outer and inner blade tip angles and rotating speed with efficiency as high as 38%, more refinement was carried out across the blade surfaces and detailed blade internals. After a series of design iterations the most optimum design was achieved with efficiency of 52%, which is close the highest possible efficiency of 59%, Ref. [9]. Figure 26 shows this design with 52% efficiency.

More study of this most optimum design was done by finding out the total power and torque as a function of rotating speed achieved with variation of wind speeds. This was done to determine a range of possible powers produced during operation when the wind blows in various speeds.

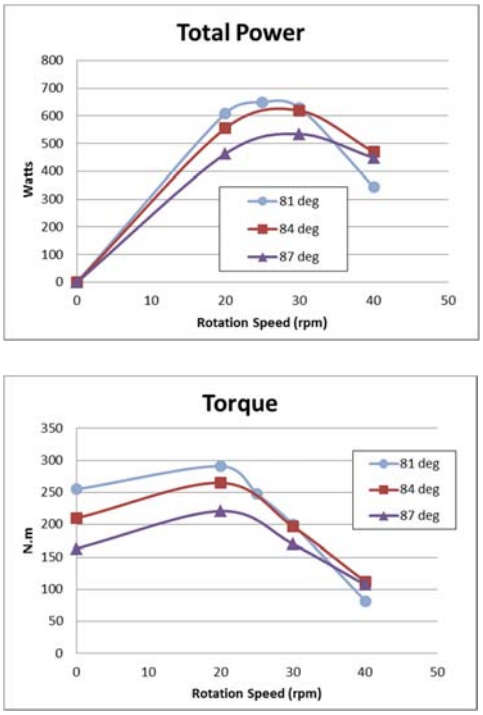

Figure-24. Power and torque as a function of rotating speeds for all outer tip angles.

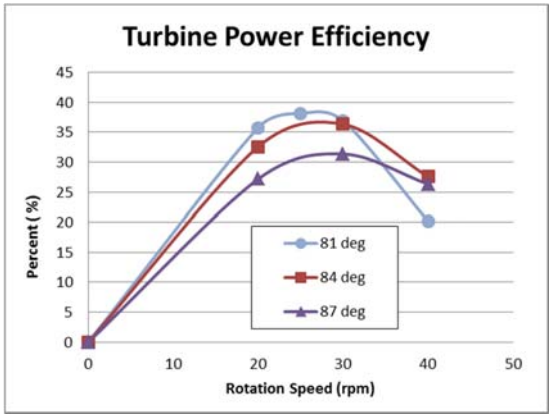

Figure-25. Wind turbine efficiency for different outer tip angles.

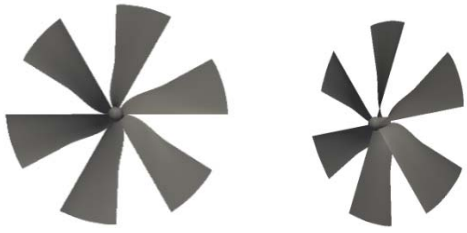

Figure-26. Wind turbine design with 52% efficiency.

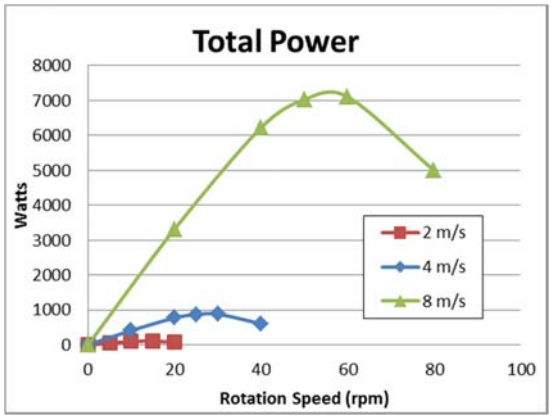

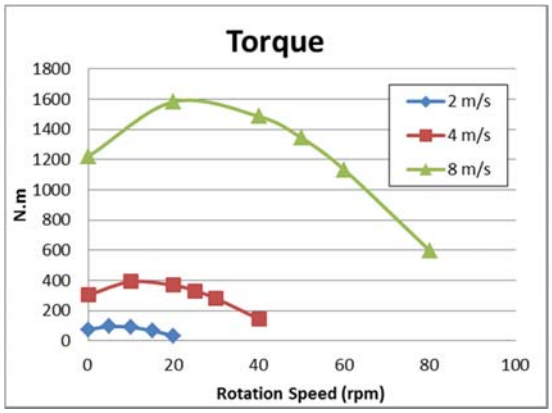

Figure-27. Power and Torque as function of rotating speed for wind speeds: 2, 4, dan 8 m/s.

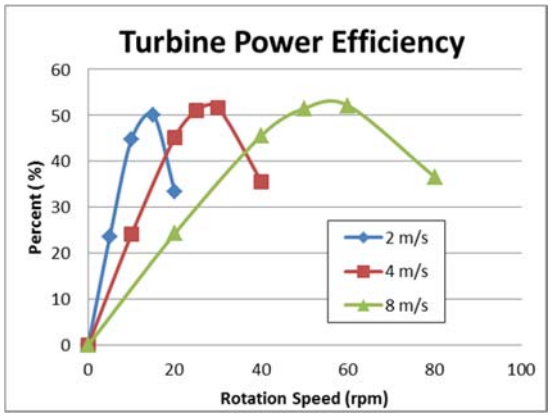

Figure-28. Wind turbine efficiency as a function of rotating speed for wind speeds: 2, 4 dan 8 m/s.

Enhanced configuration result: power and torque as a function of wind speed

Figure-27 shows power and torque produced as a function of rotating speeds with various wind speeds; 2, 4 and 8 m/s. The maximum power is shown to occur at different rotating speeds for different wind speeds. The maximum power happened at around 15 RPM for wind speed of 2 m/s. For 4 m/s wind speed the maximum power was at 30 RPM and 60 RPM for 8 m/s. It can be concluded that the maximum power is proportional to the wind speed.

For wind speed of 2 m/s, the maximum power achieved was around 100 Watts while the 4 m/s wind speed produced maximum power of 900 Watts and that of 8 m/s about 7200 Watts. Maximum torque varied with different wind speeds. For the wind speed of 2 m/s the maximum torque obtained was about 100 N.m. The wind speed of 4 m/s yields torque of about 400 N.m. The wind speed of 8 m/s produces 1600 N.m.

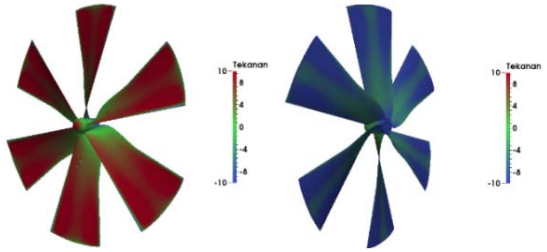

Figure-29. Pressure distribution at the front and the rear surfaces of the wind turbine for wind speed of 4 m/s and rotating speed of 30 rpm.

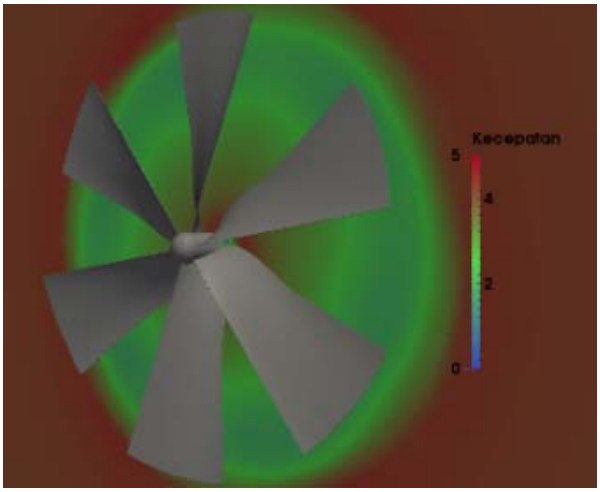

Figure-30. Velocity distribution 0.5 m downstream of the wind turbine for wind speed of 4 m/s and rotating speed of 30 rpm.

Figure-28 shows the wind turbine efficiency as a function of rotating speed for various wind speeds. The maximum efficiency is shown to occur at a rotating speed that is proportional to the wind speed. The maximum efficiency for 2, 4 and 8 m/s wind speeds occurred at 15 RPM, 30 RPM and 60 RPM, consecutively. It is

interesting to note that the maximum efficiency was almost similar for different wind speeds although the maximum power varied for different wind speeds.

Figures 29-30 show simulation result for wind speed of 4 m/s at rotating speed of 30 RPM. It can be seen that the pressure distribution at the front surface of the blades spread quite evenly showing the highest pressure of about 10 Pascal. Similarly, low pressure distribution spread evenly at the rear surface of the blades showing the lowest of -10 Pascal. This indicates that the more the pressure spread evenly at the front and the rear of the blades the higher the efficiency of the wind turbine. Figure 30 shows the wind speed at the rear surface of the blades that spread quite evenly except at the middle area, which was a little higher. This demonstrated that the efficiency could still be improved by reshaping that middle area further.

Enhanced configuration result: power and torque as function of wind "angle of attack"

Figure-31 shows the wind direction approaching the wind turbine with angle of attack β between 0º to 60º. The wind speed used was 4 m/s. This study was conducted to know the performance of the wind turbine undergoing delay in responding to the change of wind direction and/or mechanism to direct the wind turbine when its yaw controller fails to direct properly.

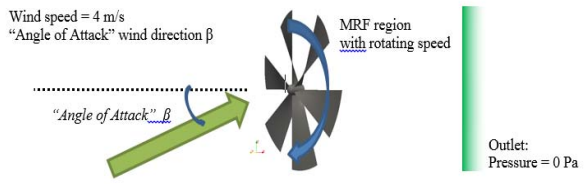

Figure-31. Simulation condition for the analysis of wind turbine.

Figure-32 shows the non-dimensional power produced by the wind turbine as a function of wind angle of attack, which ranges between 0º to 60º. The power was normalized with the power value at 0ºwind angle of attack. The curve is assumed to make symmetrical form for negative angles. There is decreasing power as much as 3% when the wind angle of attack is 10º, 10% for 20º and 30% for 30º. The power was reduced to zero when the wind angle of attack was greater than 55º.

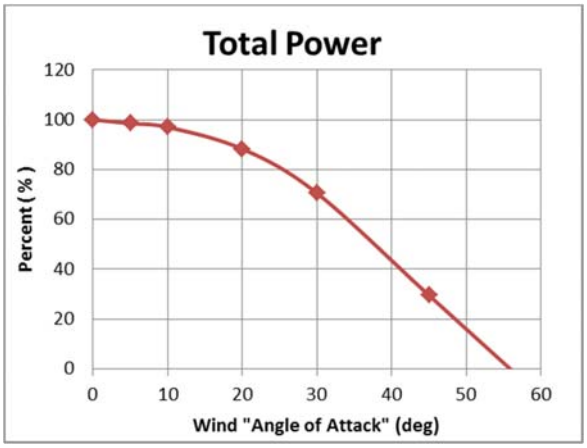

Figure-32. Normalised power as a function of wind "angle of attack".

CONCLUSIONS

The following conclusions can be drawn from the results of the presented wind turbine design and optimization:

- OpenFOAM simulation results have been validated using 3 configurations of open hemisphere producing values very close to the experimental results with up to 4% error.
- The effects of outer tip angle, inner tip angle and blade width to the total power, torque and efficiency have been evaluated as function of rotating speed in which it is found that the blade design can achieve maximum power efficiency of 36 to 38%.
- After a number of design iterations, the most optimum design of wind turbine was achieved with 52% power efficiency, which is close to the theoretical maximum efficiency (Betz limit) of 59%.
- This study shows that wind speed variation has negligible effect while wind direction (angle of attack) has significant effect to the maximum efficiency of wind turbine blade.

REFERENCES

[1] N. Sezer-Uzol, L.N. Long, "3-D Time-Accurate CFD Simulations of Wind Turbine Rotor Flow Fields," AIAA Paper No. 2006-0394.

[2] S. Gomez-Iradi, G.N. Barakos,"CFD Investigation of Wind Turbine Rotor Design Parameters," Proc. of the Institution of Mechanical Engineers, Part A: J. Power and Energy. 222(5): 455-470.

[3] C.S. Ferreira,G. van Bussel, G. van Kuik,"2D CFD simulation of dynamic stall on a vertical axis wind

turbine: verification and validation with PIV measurements," 45th AIAA Aerospace Sciences meeting and exhibit, Nevada, Reno, paper AIAA paper No. 1367.

[4] C. Kaminsky, A. Filush, P. Kasprzak, W. Mokhtar, "A CFD Study of Wind Turbine Aerodynamics," Proc. the 2012 ASEE North Central Section Conference.

[5] MS Soeripno, N. Murti, Blowing the wind energy in Indonesia. Conference and Exhibition Indonesia Renewable Energy & Energy Conservation. Indonesia EBTKE-CONEX 2013. Energy Procedia 47: 273-282.

[6] Md. Abu Abrar, A.M. Ishtiaque Mahbub, Mohammad Mamun, "Design Optimization of a Horizontal Axis Micro Wind Turbine through Development of CFD Model and Experimentation", Procedia Engineering, 90: 333-338.

[7] A. Chehouri, R. Younes, A. Ilinca, and J. Perron, "Review of performance optimization techniques applied to wind turbines", Applied Energy142: 361-388.

[8] G. Reinald Fischer, T. Kipouros, A. Mark Savill, "Multi-objective optimisation of horizontal axis wind turbine structure and energy production using aerofoil and blade properties as design variables", Renewable Energy, 62: 506-515.

[9] A.M. Biadgo, A. Simonovic, D. Komarov, S. Stupar," Numerical and Analytical Investigation of Vertical Axis Wind Turbine," FME Transactions 41.1: 49-58.

[10] OpenFOAM User Guide [Online]. Available from: http://cfd.direct/openfoam/user-guide/.

[11] F. Kreith, Y. Goswami, Ed. The CRC Handbook of Mechanical Engineering, 2nd Edition, pp 3-80, CRC Press, Boca Raton, FL.